Arabidopsis NAP1 regulates the formation of autophagosomes.

Pengwei Wang[1], Christine Richardson[1], Chris Hawes[2] and Patrick J. Hussey[1]*

1. School of Biological and Biomedical Sciences, Durham University, Durham, DH1 3LE, UK

2. Department of Biological and Medical Sciences, Oxford Brookes University, Oxford, OX3 0BP, UK

*Corresponding author: p.j.hussey@durham.ac.uk

Summary

The SCAR/WAVE complex is required for ARP2/3 mediated actin nucleation, and these complexes are highly conserved in plants and animals [1, 2]. Proteins from the SCAR/WAVE complex have been found to be membrane associated in plants [3]. Using fluorescent protein fusions we have found that NAP1 [4], a component of the SCAR/WAVE complex, locates to vesicles/puncta that appear upon applied pressure. These NAP1 vesicles can be ER associated, can co-align with the cytoskeleton and fuse to each other homotypically. More interestingly, the majority co-localizes with the autophagosome marker, ATG8 and anti-NAP1 identifies autophagosomes in immuno-TEM. Macroautophagy (hereafter referred to as autophagy) is enhanced under certain stress conditions such as nitrogen starvation and salt stress. We show that less autophagosomes are generated in the NAP1 knock-out mutant during starvation stress. The *nap1* mutant (and KO mutants of other components of the SCAR/WAVE and ARP2/3 complexes) is more susceptible to nitrogen starvation and is less salt tolerant indicating defective autophagy. In conclusion, our data show that NAP1 has another function in plant cells, other than in cell expansion, and that is as a regulator of autophagy.

Result and Discussion

Constant pressure induces the formation of NAP1-GFP puncta.

The activation of ARP2/3 complexes promotes actin filament nucleation to form branched actin networks [1-2]. In animals, a wide range of proteins (e.g Cortactin, WASP, WASH complexes) are known to be able to activate the ARP2/3 complex [5-7], however, these activator proteins are absent from plants with the exception of the SCAR/WAVE complex [8-10]. Membrane trafficking in plant cells is mainly regulated by the actin cytoskeleton [11]; however plant specific mechanisms that regulate the actin cytoskeleton-endomembrane organization are likely to exist [12-15]. Developmental defects are found when disrupting proteins from the SCAR or ARP2/3 complex in plants. These include altered cell morphogenesis, defects in root elongation and stomatal opening [10, 16-19]. All of these phenotypes must be linked to altered actin cytoskeleton activity, but the mechanisms remain unclear.

Components from the SCAR complex are membrane localised [3, 17, 20]. Here, we have focused on one protein from the SCAR complex of *Arabidopsis thaliana*, NAP1 [4]. A construct harbouring DNA encoding a NAP1: C-terminal fluorescence protein chimera was made and subsequently expressed in *Nicotiana benthamiana* leaves. NAP1-RFP localized mainly to the cytoplasm when first viewed in the normal manner, that is with a coverslip over the sample and under oil immersion conditions (Figure 1A, 0min). However, when the samples were continually imaged, NAP1-RFP labeled mobile punctate structures were observed. Their numbers increased significantly when samples were left for longer (Figure 1A). This process is better illustrated in a live cell imaging time series (Movie S1A). This phenomenon is reversible; NAP1 puncta disappeared after 30min when the cover slip was removed and the leaf segments were allowed to recover by suspension in water (Figure S1A). Interestingly, these NAP1-RFP labeled puncta were not induced when a water dipping lens (i.e. no coverslips covering the leaf sample) was used to image similar samples for the same length of time using the same laser settings (Figure 1B-C). Statistical analysis shows that the numbers of puncta identified under these two different conditions are significantly different (Figure 1D). The only variance here is the absence of cover slips (Figure 1C). We

conclude from these data that the constant pressure caused by the oil immersion lens and cover slips trigger the formation of the NAP1-RFP puncta.

In order to determine whether NAP1 is acting alone or as part of its complex (e.g. SCAR/WAVE and APR2/3), we co-expressed constructs harbouring GFP-SCAR2 or RFP-ARP3 with NAP1-XFP (GFP or RFP). On their own, the GFP-SCAR2 and the RFP-ARP3 localized to the cytoplasm in the *N. benthamiana* leaf epidermal cells when treated with constant pressure by the coverslip (Figure 1E, G). However, when co-expressed with the NAP1-XFP, both the SCAR2 and the ARP3 were recruited to the pressure induced NAP1 puncta. This indicates that NAP1 which is associated with the induced puncta can form a complex with other components of the SCAR/WAVE complex and also interact with a marker for the ARP2/3 complex. Both complexes being located at the same place suggest that they can potentially function to activate actin polymerization (Figure 1I).

The majority of the NAP1-XFP puncta associate with ER membrane (95.3 ± 5.5%), actin filaments (79.9 ± 4.1%) and microtubules (96.1 ± 6.9%; Figure 1J-L); dual associations with the actin cytoskeleton and the ER are also seen (Figure 1J). Previous studies have shown that the ARP2/3 subunit, ARPC2, binds microtubules and localizes to punctate structures in plants [21]. Moreover, an animal WASP homologue WHAMM has also been shown to be microtubule associated [6]. Therefore, dual association of the ARP2/3 complex or its activating proteins with the actin-microtubule cytoskeleton is likely to be a general phenomenon in eukaryotic cells.

Effect of pressure on endogenous Arabidopsis NAP1

The main defect in the Arabidopsis *nap1* mutant is distorted trichomes (Figure 2A-B) [3, 9-10]. We generated a construct whereby the expression of NAP1-GFP would be driven by its endogenous promoter (Pro::NAP1-GFP). The *nap1* mutant was transformed with the Pro::NAP1-GFP construct and its expression resulted in the complementation of the trichome phenotype (Figure 2C), indicating that the NAP1-GFP protein chimera used in this study is functional. Moreover, the NAP1-GFP was enriched at cell corners in roots (Fig. 2E), which is a similar localization to other SCAR complex proteins, e.g. PIR121, BRICK1 [3]. In leaf pavement cells the NAP1-GFP also labels punctate structures in the cytoplasm (Figure 2 D).

Next, we raised an antibody to Arabidopsis NAP1 and performed localization studies for the endogenous Arabidopsis NAP1. The anti-NAP1 was tested for its specificity. It detects a clear band at the appropriate molecular weight on 1D gel immunoblots of extracts from Arabidopsis seedlings and from *N. benthamiana* leaves expressing NAP1-GFP (Figure 2G-H). Arabidopsis leaf tissue was prepared for immunolocalization of NAP1 using the antibody by freeze-shattering. The anti-NAP1 labelled ER-associated punctate structures (Figure 2J). These data indicate that the endogenous NAP1 localization is the same as the NAP1-GFP localization in either *N. Benthamiana* (Figure 1J) or Arabidopsis (Figure 2D). As a further control to the specificity of anti-NAP1, the anti-NAP1 was used on root tissue from *nap1* mutants and no labeling was observed (Figure 2K).

Immunofluorescence studies on Arabidopsis root tip cells revealed that most of the anti-NAP1 staining was cytoplasmic with few puncta identified under normal conditions (Figure 2L). When the root tissue was treated with constant pressure (using cover slips as in Figure 1C for 20-30min) before fixation, anti-NAP1 labeled punctate structures and these were much more abundant (Figure 2M). These results show the endogenous NAP1 behaves in the same way as NAP1-GFP, in terms of its localization and response to external pressure.

NAP1 localizes to double-membrane structures and co-localizes with ATG8

The next question we addressed was to establish what the nature of these NAP1 puncta are. This was attempted by co-expressing the NAP1-XFP construct with constructs encoding various organelle markers; ST-RFP for Golgi, VAP27-1-YFP for ER-PM contact sites, VTI12-mCherry for pre-vacuolar compartments and RabF2a-mCherry for the *trans*-Golgi network. Apart from some co-localisation with VAP27-1-YFP at the ER-PM contact sites, no other co-localisation was observed (Figure S1B-F).

We then performed immunogold labeling of Arabidopsis root tips using anti-NAP1 gold particles and these localized to the plasma membrane, and ER associated double-membrane structures that encapsulate other cytoplasm components. These structures are reminiscent of autophagosomes (Figure 2F). The anti-NAP1 gold particles were found mostly at the PM, autophagosome-like structures and other membrane vesicles (Figure 2F). The enrichment of anti-NAP1 gold particles at autophagosome-like structures is further confirmed statistically using chi-square tests (Figure 2I).

Autophagy is a regulated mechanism that allows cells to degrade their own cytoplasmic constituents. This pathway can be enhanced under stress conditions [22, 23]. Autophagy is also essential during plant development and embryogenesis [24]. Membranes used in autophagosome biogenesis may originate from various compartments but the best studied is where the ER network is involved [25]. Autophagy is regulated by a group of autophagy-related proteins [26], and ATG8 is the commonly used marker for autophagosomes [27]. When constructs encoding YFP-ATG8 and NAP1-GFP were co–expressed in leaf epidermal cells, ATG8 labelled autophagosomes were observed and a proportion of these co-localise with NAP1-GFP puncta (Figure 3A). After 20-30min pressure the majority of the punctae were labelled with both NAP1-GFP and YFP-ATG8 (65.4 ± 12.8%; Figure 3B). Co-localization of RFP-SCAR2 and NAP1-GFP with the autophagosome marker YFP-ATG8 is also found (Figure S2A). Interestingly, a previous study has demonstrated that autophagy can be induced by mechanical stress in Dictyostelium [28]. According to this previous study, autophagosome formation appears after 10-30mins of applied pressure, and this length of time is in agreement with the observations we have made here.

Hydrogen peroxide is known to trigger the formation of autophagosomes [29]. When *N. benthamiana* leaf epidermal cells or Arabidopsis hypocotyl cells expressing NAP1-GFP were treated with H_2O_2 a significant number of NAP1 puncta were formed which either co-labelled with YFP-ATG8 (Figure 3C) or MDC (Monodansylcadaverine, an autophagosome dye; Figure S2C). Therefore, we propose that these NAP1-GFP labelled puncta (hereafter referred as NAP1 labelled autophagosomes) are autophagosomes and these are formed either upon mechanical stress or oxidative stress induced by H_2O_2.

Nutrient depletion also enhances the autophagic pathway [30]. Large numbers of autophagosomes in leaf epidermal cells are formed when Arabidopsis plants harbouring a construct encoding GFP-ATG8 are grown in medium without nitrogen (Figure 3D, F). The same nitrogen deprivation (-N) stress is also able to trigger the formation of NAP1-GFP labelled autophagosomes (Figure 3E-F). These observations are in agreement with previous studies on starvation induced autophagy [22,30]. These root cells were fixed and immuno-labelled with an ATG8 antibody [26] and the endogenous ATG8 co-localized with the NAP1-GFP at autophagosomes (Figure S2B). Concanamycin A (Con A) blocks the V-ATPase activity at the tonoplast and, as a result, the degradation ability of the vacuole is inhibited [30].

When NAP1-GFP plants were grown on –N medium and treated with Con A, membranes labelled with NAP1-GFP were found inside the vacuole (Figure S2D, arrow), which is similar to the behaviour of other known autophagosome proteins when cells are treated in this way [22, 31].

These data indicate that NAP1 (and possibly the SCAR-ARP2/3 complexes) is required for the formation of autophagosomes under certain stress conditions. Together these proteins are able to nucleate actin polymerization which could potentially provide the forces needed for membrane deformation during the phagophore stage [32] and/or the actin polymerisation resulting from the activity of the two complexes could be involved in the trafficking of autophagosomes to the lytic compartment [33].

The formation of pressure induced autophagosomes requires homotypic fusion and sequential recruitment of NAP1 and ATG8.

NAP1-GFP puncta are formed 9 min after applying constant pressure. At this stage, the YFP-ATG8 signal is mostly found in the cytoplasm. It is only after 18min that the YFP-ATG8 is recruited to the autophagosomes (Figure 3G). We further quantified this process by analyzing the change in fluorescence signal intensity at the different time points; the YFP-ATG8 signal starts to accumulate on puncta at 20min, much later than the NAP1-GFP signal which increases at 9min (Figure 3H-I). These observations indicate that NAP1 is recruited to the ER membrane in the first instance, possibly regulating actin polymerization and formation of phagophores, which then later develop into mature autophagosomes with ATG8 incorporated.

NAP1-GFP puncta can fuse to each other, and their size increases after each homotypic fusion event. As illustrated in Figure 3J, two NAP1-GFP puncta fuse at 0-24s, generating a larger structure which later fuses with another puncta at 90-114s (Figure 3J). Statistical analysis indicates that the average size of NAP1-GFP puncta increased over time and they reach a maximum of 1 μm at approximately 20min (Figure 3K); the number of puncta, however, decreased over time (Figure 3L) which is likely to be due to the fusion events.

The Arabidopsis *nap1* mutant is defective in autophagy, and more susceptible to nitrogen starvation and high salt stress

If NAP1 is involved in autophagy as our results strongly suggest, then we would expect an autophagy phenotype for the *nap1* mutant and perhaps other SCAR/WAVE or ARP2/3 complex mutants. We used anti-ATG8 for immuno-fluorescence studies in Arabidopsis wild-type and the *nap1* mutant. Under normal growth conditions, few autophagosomes could be identified (Figure 4A), however, their number increased dramatically when plants were grown in nitrogen dropout medium (-N) for 2 days (Figure 4B). As expected, these anti-ATG8 labeled autophagosomes were associated with the ER membrane (Figure 4D). However, the formation of autophagosomes in the *nap1* mutant is prevented during N starvation; their numbers were significantly lower compared to wild type (Figure 4C, F). This result suggests that the formation of autophagosomes is regulated by NAP1. As a result of an impaired autophagy pathway, plant development and root growth in the *nap1* mutant grown under nitrogen starvation is affected more severely than in the wild type (Figure 4E). The size of the *nap1* seedling was smaller, and their roots were much shorter than wild type (Figure 4G). The Arabidopsis NAP1-GFP complemented plants exhibit a wild type phenotype when similarly grown under nitrogen starvation. This line is heterozygous and allowed us to see complemented (arrow) and non-complemented (arrow head) phenotypes on the same plate (Figure 4E). A similar study was also performed using other KO mutants, such as *arp2*, *pir121* and *atg5* (an autophagy mutant) under N starvation. Using *pir121* as an example, retarded root development (Figure S3A-B) and reduced autophagosome formation (Figure S3C) is also found.

Salinity stress is also known to enhance autophagic activity in plants [23]. We show here that numerous NAP1-GFP labeled autophagosomes form when plants are grown in medium containing high concentrations of NaCl (160mM; Figure S2E-F). The salt tolerance of the Arabidopsis *nap1* mutant was tested together with other mutants of SCAR and ARP2/3 complex proteins, namely *pir121, scar2* and *arp2* knock-out lines. Forty plants were analyzed for each line. The number of susceptible (-) and non-susceptible (+) plants under salt stress were scored (Figure 4I). The result shows that as well as the *nap1* mutant, *pir121* and *arp2* are also susceptible to salt stress. The *scar2* mutant is not which is likely to be because of functional redundancy between the four SCAR genes [9, 10]. NAP1, PIR121 and ARP2 are single copy genes [34]. Moreover, the Arabidopsis NAP1 complemented plants exhibit a similar salt tolerance to wild type (Figure 4K-H). In summary, we have

demonstrated that the Arabidopsis *nap1* mutant is defective in autophagy, as a consequence, its development is perturbed under certain stress conditions where elevated autophagy is required.

A model of NAP1 regulated autophagy

Previous studies using animal cells and yeast have demonstrated that the actin cytoskeleton participates in the early events of autophagosome formation [35]. Taking these data together with the data presented here, a new model for the formation of autophagosomes is proposed (Figure 4J). Upon certain stimulation (e.g. pressure), NAP1 proteins are recruited to the ER membrane from the cytoplasm (1). ER associated NAP1 activates actin polymerization and drives membrane deformation, facilitating phagophore formation and expansion (2-3). At a later stage, ATG8 is recruited to the phagophore and gradually forms the mature autophagosome (3-4). The cytoskeleton is found closely associated with NAP1 and autophagosome membrane and this provides the force for membrane deformation and the track for autophagosome transport (4). Finally, autophagosomes are transported to the vacuole, where they are internalised and become degraded (5)

In conclusion, we have demonstrated that constant pressure can induce NAP1 to localise to autophagosomes. The majority of them are ER associated, and co-align with actin filaments and microtubules. The recruitment of NAP1 and ATG8 to the phagophore/autophagosome happens sequentially, and homotypic fusions of these puncta are seen at an early stage of autophagosome formation. The Arabidopsis *nap1* mutant is defective in autophagy and as a result, it is more susceptible to nitrogen starvation and is less salt tolerant. A similar phenotype is also seen in other Arabidopsis mutants lacking key regulatory proteins of SCAR/WAVE or ARP2/3 complex. Therefore, a novel function of NAP1 in autophagy is reported here.

Figure legends

Figure 1. Fluorescence protein tagged NAP1 is recruited to cytoplasmic punctate structures in *N.benthamiana* leaf epidermal cells after pressure induced by cover slips.

(A) NAP1-RFP initially localises to the cytoplasm after mounting the leaf tissue on the microscope slide with cover slips (0 min). The constant pressure exerted by the coverslip whilst imaging induces the formation of punctate structures that are labelled by NAP1-RFP. They start to appear at around 6min, and their number increase up to 17min. **(B)** In contrast, NAP1-GFP remains cytoplasmic when imaging with a water-dipping lens, and few punctate structures can be seen. **(C)** Illustration of different sample preparations: no cover slips are used with a water dipping lens, therefore cells in (b) do not suffer from constant pressure as in (a). **(D)** Statistical analysis of NAP1-RFP puncta. Their number is higher under the pressure of cover slips (20min) and such structures disappear when such pressure is removed. **(E)** RFP-ARP3 localises to the cytoplasm, no puncta are induced under the same pressured conditions as in (a). **(F)** In the presence of NAP1-GFP and constant pressure, RFP-ARP3 is also recruited to the NAP1-GFP labelled puncta. **(G-H)** Similarly, cytoplasmic GFP-SCAR2 co-localises with NAP1-RFP on the puncta after pressure. **(I)** Simplified illustration of the SCAR and ARP2/3 complex. NAP1 together with other regulatory proteins, namely, PIR121, BRK1 and ABI, activate the SCAR proteins and facilitate actin polymerization through the ARP2/3 complex. **(J)** In order to form NAP1 puncta, samples were applied with constant pressure for 20min before imaging. A number of NAP1-GFP labelled puncta associate with actin filaments (GFP-Lifact) and the ER network (CFP-HDEL), the percentage of association is calculated as 79.9±4.1% and 95.3±5.5% respectively. **(K)** The association between NAP1-RFP puncta with microtubules is 96.1±6.9%. **(L)** Statistical analysis of NAP1 puncta with actin, microtubules and ER network (scale bar = 10 μm). See also Figure S1 and Movie S1.

Figure 2. Localisation of NAP1 in Arabidopsis

(A-B) The *nap1* knock-out mutant exhibits distorted trichomes **(C)** The defective trichome in *nap1* mutants is rescued by stably expressing NAP1-GFP driven by its endogenous promoter (Pro::NAP1-GFP). **(D)** Arabidopsis leaf epidermal cells expressing NAP1-GFP (the same lines as in C), which localises to cytoplasm and punctate structures. However, its signal is enriched at the corners. **(E)** The localization of Pro::NAP1-GFP in root tips with a polarised distribution at cell junctions and enrichment at cell corners. **(F)** TEM and Immuno-gold labelling of endogenous NAP1 in Arabidopsis root tips. Gold particles localise to the plasma membrane, as well as to double membrane structures reminiscent of autophagosomes. In addition, NAP1 gold particles were found in the cytoplasm and vesicle-related structures. Their occurrence is given in the table (counted from 20 images). **(G)** Western blot of total Arabidopsis seedling protein extract probed with a polyclonal NAP1 antibody showing a clear band at ca. 120 kDa. **(H)** Western blot of protein extracts from *N. benthaminana*

expressing NAP1-GFP. NAP1 (1) and GFP (2) antibodies were used on two different strips; both antibodies detect a band at 150kDa which represents NAP1-GFP. **(I)** Analysis of NAP1 gold particle (in image F) association with the PM using chi-square tests. The distribution of NAP1 gold was scored as PM/autophagosome-associated or non-associated over 6.79µm^2. The association of NAP1 on the PM is significantly different from that were the distribution to be random ($p<0.0001$). Similarly, the distribution of NAP1 gold with autophagosomes was performed in the same way. **(J)** Immuno-fluorescence of Arabidopsis leaf epidermal cells with NAP1 (TRITC, red) and BIP2 (FITC, green) antibodies. Endogenous NAP1 localises to ER associated puncta as well as the cytoplasm. **(K)** Immuno-fluorescence of Arabidopsis roots of the *nap1* knock-out mutant. No labelling can be detected when using the NAP1 antibody. **(L-M)** Immunofluorescence of Arabidopsis roots expressing GFP-HDEL with NAP1 (TRITC, red) antibody. Roots in (M) were treated with constant pressure for 20-30min before fixation. Endogenous NAP1 was found on punctate structures that associate with the ER membrane (better illustrated in the zoomed image, in-set). In contrast, few puncta were found when roots were fixed without pressure pretreatment (L) (Scale bar = 10 µm; 500nm for TEM).

Figure 3. NAP1-GFP labelled puncta are identified as autophagosomes.

N. benthamiana leaf epidermal cells co-expressing NAP1-GFP and YFP-ATG8e which labels autophagosomes (A,B,C and G). (A) Most of the NAP1-GFP signal is found in the cytoplasm before the cells were treated with prolonged pressure . NAP1 puncta can be identified but are low in abundance and some co-localise with an autophagosome marker (ATG8, arrow). **(B)** More NAP1 labelled puncta are induced when cells are treated with constant pressure for 20-30min. High frequency (65.4 ± 12.8%) of co-localization with YFP-ATG8 can be seen, and NAP1 puncta free of YFP-ATG8 are also observed (arrow). Inset picture shows the co-localization between two proteins at a low detection setting. **(C)** When cells are treated with H_2O_2, NAP1 and ATG8 puncta are induced and most co-localize. Inset picture shows the co-localization of a selected area with higher magnification **(D)** Autophagosomes form when Arabidopsis plants are growing in medium minus nitrogen. In leaf epidermal cells, the number of autophagosomes labelled by GFP-ATG8 dramatically increases under nitrogen starvation. **(E)** Interestingly, the number of NAP1-GFP puncta in Arabidospsis roots also increases when nitrogen is removed from the medium. **(F)** Statistical analysis on the number of NAP1-GFP and GFP-ATG8 labelled autophagosomes from (d and e). A significant increase is seen under starvation conditions. **(G)** Time series from a *N. benthamiana* leaf segment expressing NAP1-GFP and YFP-ATG8 mounted with a cover slip. NAP1 puncta can be seen after approximately 9mins; but the appearance of autophagosomes (YFP-ATG8 labelled) is only seen at a later stage, after 18mins. Inset picture shows the co-localization of NAP1-GFP and YFP-ATG8 in a selected area. **(H-I)** Statistical study of the fluorescence intensity of puncta labelled with NAP1-GFP or YFP-ATG8 from (g). Cytoplasmic fluorescence is measured if no puncta could be identified (e.g. NAP1 at 0min; ATG8 at 0-13min). Fluorescence

intensity of these puncta increases with time. **(J)** Homotypic fusion of NAP1-GFP puncta in *N.benthamiana* leaves. Note the punctum at 0 second (arrow) fuses with an adjacent one at 18s, and its size increases after fusion. The same punctum later fuses again with two other puncta at 90-114 seconds. **(K)** At different time points, the size of NAP1 puncta were measured; their size appears to increase with time. **(L)** Statistical analysis of the number of puncta formed at different time points. (Scale bar = 10 µm). See also Figure S1 and S2.

Figure 4. Arabidipsis *nap1* mutants are defective in the autophagic pathway.

(A-C) Immuno-fluorescence of Arabidopsis leaf epidermal cells with the ATG8 (TRITC, red) antibody. Autophagosomes are induced after nitrogen starvation in wild type Arabidopsis. However, their number reduces significantly in the *nap1* knock-out mutant. **(D)** Immuno-fluorescence of GFP-HDEL (ER) expressing Arabidopsis leaf epidermal cells with ATG8 (TRITC, red) antibody. **(E)** Arabidopsis *nap1* mutant grown in nitrogen dropout medium exhibits slow development and shorter roots (7 days after germination). In contrast, such an effect is less noticeable in wild type and NAP1-GFP complemented plants. **(F)** Statistical analysis of the number of autophagosomes as described in (B-D). For each cell after N starvation, 17.9 ± 6.6 autophagosomes are found in wild type, and 6.3 ± 2.3 in the *nap1* mutant. **(G)** Measurement of Arabidopsis root length in (E; unit/mm). Significant reduction in root length can be seen in the *nap1* mutant. **(K-H)** Autophagy is required for tolerance of salt stress in plants. A collection of SCAR and Arp2/3 mutants were used: *nap1*, *pir121*, *scar2* and *arp2.* They were grown on normal half MS medium as well as in medium containing high NaCl (160mM) for 6 days. **(I)** Proposed model of NAP1 regulated autophagy. (Scale bar = 10 µm). See also Figure S3.

Authors Contribution

P.W. and P.J.H designed and planned the research. P.W. performed the research and wrote the manuscript with P.J.H., C.H. contributed to data analysis and manuscript editing. C.R. performed fixation and EM studies.

Acknowledgements

We thank Diane Bassham, Iowa State University for providing the GFP-ATG8 construct and Arabidopsis. We also appreciate the help from Helen Grindley on SEM experiments, and useful discussions with Michael Deeks, Susanna Pollastri and Marc Knight throughout the project.

References

1. Davidson, A.J., and Insall, R.H. (2011). Actin-based motility: WAVE regulatory complex structure reopens old SCARs. Curr Biol 21, R66-68.

2. Deeks, M.J., and Hussey, P.J. (2005). Arp2/3 and SCAR: plants move to the fore. Nat Rev Mol Cell Biol 6, 954-964.

3. Dyachok, J., Shao, M.R., Vaughn, K., Bowling, A., Facette, M., Djakovic, S., Clark, L., and Smith, L. (2008). Plasma membrane-associated SCAR complex subunits promote cortical F-actin accumulation and normal growth characteristics in Arabidopsis roots. Molecular plant 1, 990-1006.

4. Deeks, M.J., Kaloriti, D., Davies, B., Malho, R., and Hussey, P.J. (2004). Arabidopsis NAP1 is essential for Arp2/3-dependent trichome morphogenesis. Curr Biol 14, 1410-1414.

5. Derivery, E., Sousa, C., Gautier, J.J., Lombard, B., Loew, D., and Gautreau, A. (2009). The Arp2/3 activator WASH controls the fission of endosomes through a large multiprotein complex. Dev Cell 17, 712-723.

6. Campellone, K.G., Webb, N.J., Znameroski, E.A., and Welch, M.D. (2008). WHAMM is an Arp2/3 complex activator that binds microtubules and functions in ER to Golgi transport. Cell 134, 148-161.

7. Weaver, A.M., Heuser, J.E., Karginov, A.V., Lee, W.L., Parsons, J.T., and Cooper, J.A. (2002). Interaction of cortactin and N-WASp with Arp2/3 complex. Curr Biol 12, 1270-1278.

8. Le, J., Mallery, E.L., Zhang, C., Brankle, S., and Szymanski, D.B. (2006). Arabidopsis BRICK1/HSPC300 is an essential WAVE-complex subunit that selectively stabilizes the Arp2/3 activator SCAR2. Curr Biol 16, 895-901.

9. Uhrig, J.F., Mutondo, M., Zimmermann, I., Deeks, M.J., Machesky, L.M., Thomas, P., Uhrig, S., Rambke, C., Hussey, P.J., and Hulskamp, M. (2007). The role of Arabidopsis SCAR genes in ARP2-ARP3-dependent cell morphogenesis. Development 134, 967-977.

10. Zhang, C., Mallery, E.L., Schlueter, J., Huang, S., Fan, Y., Brankle, S., Staiger, C.J., and Szymanski, D.B. (2008). Arabidopsis SCARs function interchangeably to meet actin-related protein 2/3 activation thresholds during morphogenesis. Plant Cell 20, 995-1011.

11. Boevink, P., Oparka, K., Santa Cruz, S., Martin, B., Betteridge, A., and Hawes, C. (1998). Stacks on tracks: the plant Golgi apparatus traffics on an Actin/ER network. Plant J 15, 441-447.

12. Deeks, M.J., Calcutt, J.R., Ingle, E.K., Hawkins, T.J., Chapman, S., Richardson, A.C., Mentlak, D.A., Dixon, M.R., Cartwright, F., Smertenko, A.P., et al. (2012). A superfamily of actin-binding proteins at the actin-membrane nexus of higher plants. Curr Biol 22, 1595-1600.

13. Wang, P., Hawkins, T.J., Richardson, C., Cummins, I., Deeks, M.J., Sparkes, I., Hawes, C., and Hussey, P.J. (2014). The plant cytoskeleton, NET3C, and VAP27 mediate the link between the plasma membrane and endoplasmic reticulum. Curr Biol 24, 1397-1405.

14. Wang, P., and Hussey, P.J. (2015). Interactions between plant endomembrane systems and the actin cytoskeleton. Frontiers in plant science 6, 422.

15. Wang, P., Richardson, C., Hawkins, T.J., Sparkes, I., Hawes, C., and Hussey, P.J. (2016). Plant VAP27 proteins: domain characterization, intracellular localization, and role in plant development. New Phyt, DOI: 10.1111/nph.13857

16. Zhang, X., Dyachok, J., Krishnakumar, S., Smith, L.G., and Oppenheimer, D.G. (2005). IRREGULAR TRICHOME BRANCH1 in Arabidopsis encodes a plant homolog of the actin-related protein2/3 complex activator Scar/WAVE that regulates actin and microtubule organization. Plant Cell 17, 2314-2326.

17. Dyachok, J., Zhu, L., Liao, F., He, J., Huq, E., and Blancaflor, E.B. (2011). SCAR mediates light-induced root elongation in Arabidopsis through photoreceptors and proteasomes. Plant Cell 23, 3610-3626.

18. Jiang, K., Sorefan, K., Deeks, M.J., Bevan, M.W., Hussey, P.J., and Hetherington, A.M. (2012). The ARP2/3 complex mediates guard cell actin reorganization and stomatal movement in Arabidopsis. Plant Cell 24, 2031-2040.

19. Zhao, Y., Pan, Z., Zhang, Y., Qu, X., Zhang, Y., Yang, Y., Jiang, X., Huang, S., Yuan, M., Schumaker, K.S., et al. (2013). The actin-related Protein2/3 complex regulates mitochondrial-associated calcium signaling during salt stress in Arabidopsis. Plant Cell 25, 4544-4559.

20. Zhang, C., Mallery, E., Reagan, S., Boyko, V.P., Kotchoni, S.O., and Szymanski, D.B. (2013). The endoplasmic reticulum is a reservoir for WAVE/SCAR regulatory complex signaling in the Arabidopsis leaf. Plant physiology 162, 689-706.

21. Havelkova, L., Nanda, G., Martinek, J., Bellinvia, E., Sikorova, L., Slajcherova, K., Seifertova, D., Fischer, L., Fiserova, J., Petrasek, J., et al. (2015). Arp2/3 complex subunit ARPC2 binds to microtubules. Plant Sci 241, 96-108.

22. Klionsky, D.J., Abdalla, F.C., Abeliovich, H., Abraham, R.T., Acevedo-Arozena, A., Adeli, K., Agholme, L., Agnello, M., Agostinis, P., Aguirre-Ghiso, J.A., et al. (2012). Guidelines for the use and interpretation of assays for monitoring autophagy. Autophagy 8, 445-544.

23. Liu, Y., Xiong, Y., and Bassham, D.C. (2009). Autophagy is required for tolerance of drought and salt stress in plants. Autophagy 5, 954-963.

24. Minina, E.A., Filonova, L.H., Fukada, K., Savenkov, E.I., Gogvadze, V., Clapham, D., Sanchez-Vera, V., Suarez, M.F., Zhivotovsky, B., Daniel, G., et al. (2013). Autophagy and metacaspase determine the mode of cell death in plants. J Cell Biol 203, 917-927.

25. Le Bars, R., Marion, J., Le Borgne, R., Satiat-Jeunemaitre, B., and Bianchi, M.W. (2013). ATG5 defines a phagophore domain connected to the endoplasmic reticulum during autophagosome formation in plants. Nature communications 5, 4121.

26. Ketelaar, T., Voss, C., Dimmock, S.A., Thumm, M., and Hussey, P.J. (2004). Arabidopsis homologues of the autophagy protein Atg8 are a novel family of microtubule binding proteins. FEBS Lett 567, 302-306.

27. Contento, A.L., Xiong, Y., and Bassham, D.C. (2005). Visualization of autophagy in Arabidopsis using the fluorescent dye monodansylcadaverine and a GFP-AtATG8e fusion protein. Plant J 42, 598-608.

28. King, J.S., Veltman, D.M., and Insall, R.H. (2011). The induction of autophagy by mechanical stress. Autophagy 7, 1490-1499.

29. Xiong, Y., Contento, A.L., Nguyen, P.Q., and Bassham, D.C. (2007). Degradation of oxidized proteins by autophagy during oxidative stress in Arabidopsis. Plant physiology 143, 291-299.

30. Bassham, D.C. (2015). Methods for analysis of autophagy in plants. Methods 75, 181-188.

31. Zhuang, X., Wang, H., Lam, S.K., Gao, C., Wang, X., Cai, Y., and Jiang, L. (2013). A BAR-domain protein SH3P2, which binds to phosphatidylinositol 3-phosphate and ATG8, regulates autophagosome formation in Arabidopsis. Plant Cell 25, 4596-4615.

32. Kast, D.J., Zajac, A.L., Holzbaur, E.L., Ostap, E.M., and Dominguez, R. (2015). WHAMM Directs the Arp2/3 Complex to the ER for Autophagosome Biogenesis through an Actin Comet Tail Mechanism. Curr Biol 25, 1791-1797.

33. Monastyrska, I., He, C., Geng, J., Hoppe, A.D., Li, Z., and Klionsky, D.J. (2008). Arp2 links autophagic machinery with the actin cytoskeleton. Mol Biol Cell 19, 1962-1975.

34. Szymanski, D.B. (2005). Breaking the WAVE complex: the point of Arabidopsis trichomes. Curr Opin Plant Biol 8, 103-112.

35. Aguilera, M.O., Beron, W., and Colombo, M.I. (2012). The actin cytoskeleton participates in the early events of autophagosome formation upon starvation induced autophagy. Autophagy 8, 1590-1603.

A. NAP1-RFP (+ cover slips)

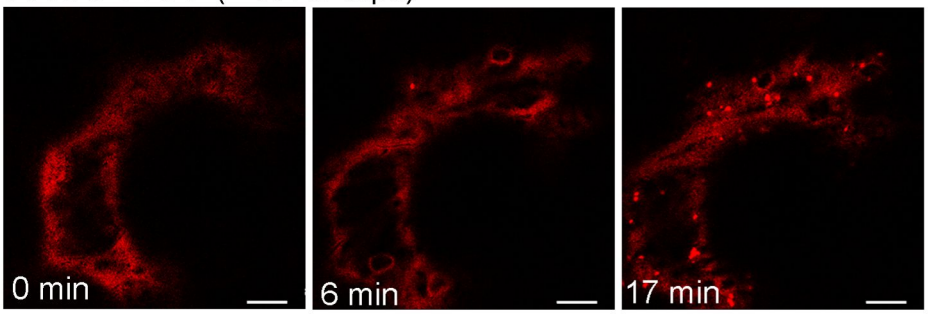

B. NAP1-RFP, water dipping lens (- cover slips)

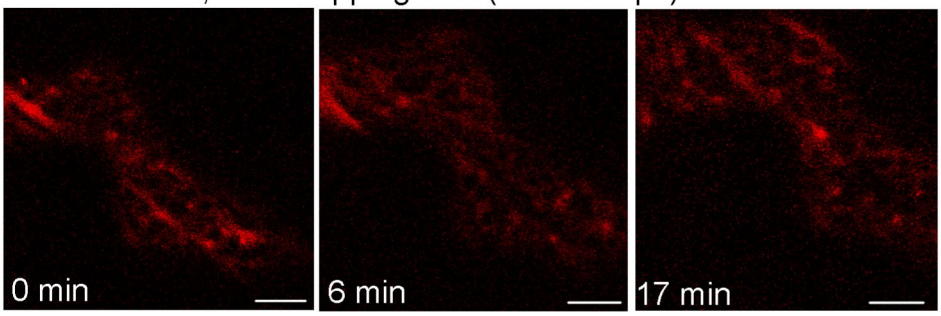

C.

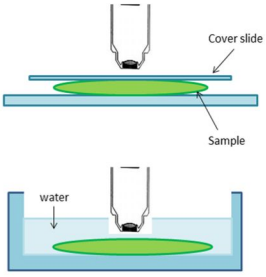

+cover slip, constant pressure

-cover slip, water-dipping lens, no pressure

D.

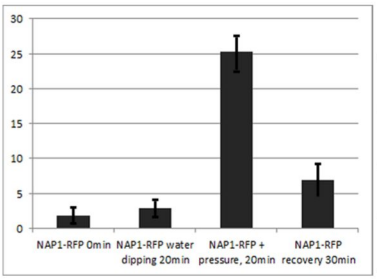

NAP1-RFP, 0min	1.8± 1.1
NAP1-RFP + pre,20min	2.9± 1.5
NAP1-RFP + water,20min	25.3 ± 3.6
NAP1-RFP, rec,30min	6.9± 3.3

+20min pressure

E. RFP-ARP3, only

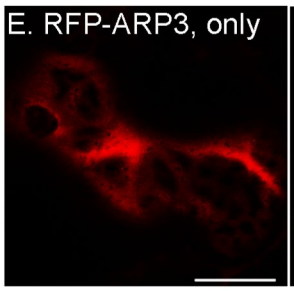

F. NAP1-GFP

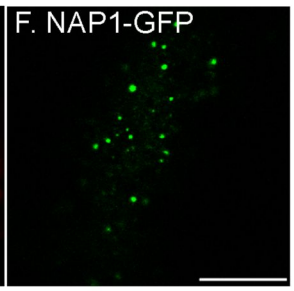

RFP-ARP3

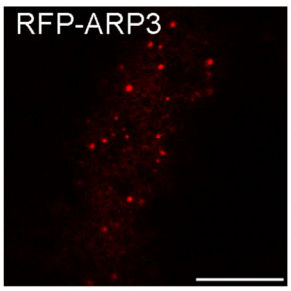

Merge

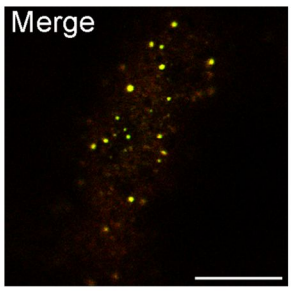

G. GFP-SCAR2, only

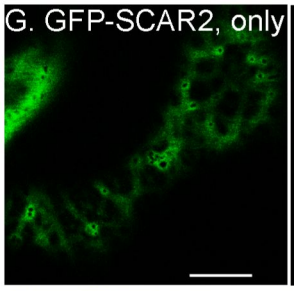

H.NAP1-RFP

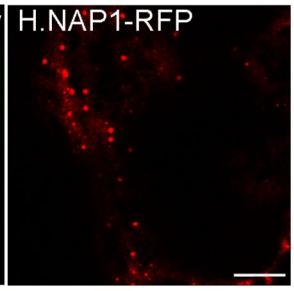

GFP-SCAR2

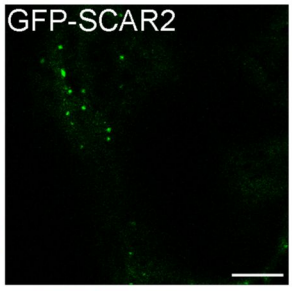

Merge

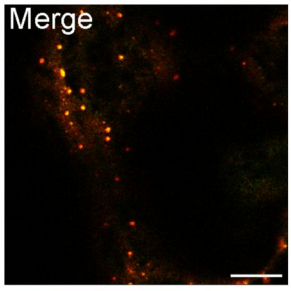

I.

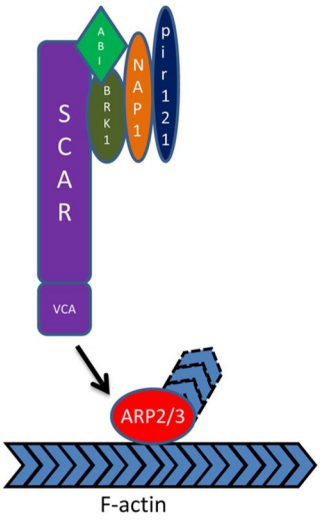

J. CFP-HDEL

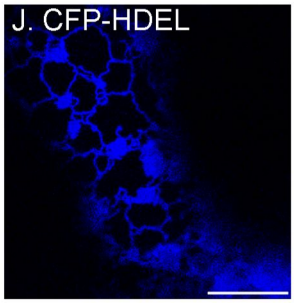

NAP1-GFP

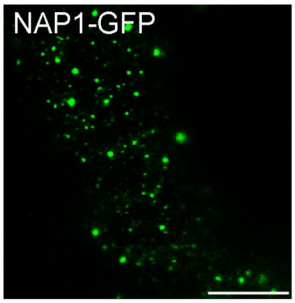

RFP-Lifact

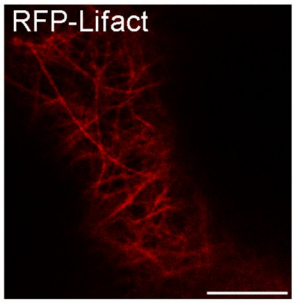

NAP1 + Lifact

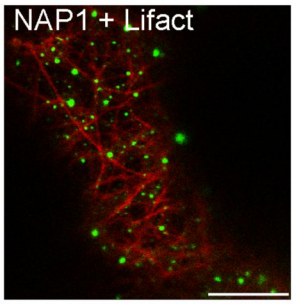

Merge

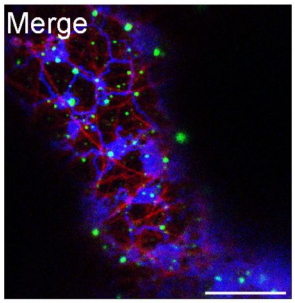

K. NAP1-RFP

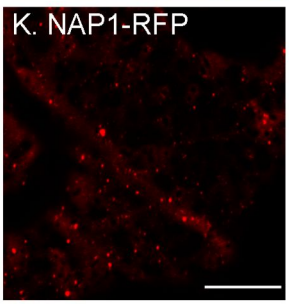

GFP-KMD

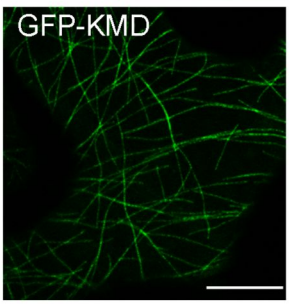

Merge

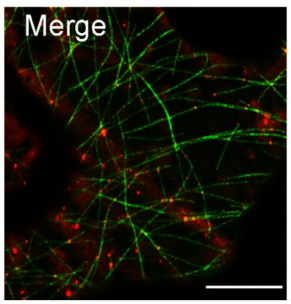

L.

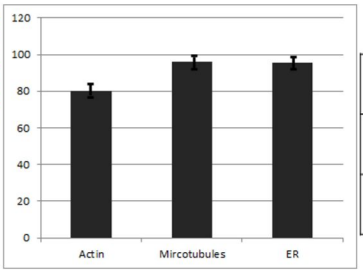

Actin	79.9 ± 4.1
Microtubules	96.1 ± 6.9
ER network	95.3 ± 5.5

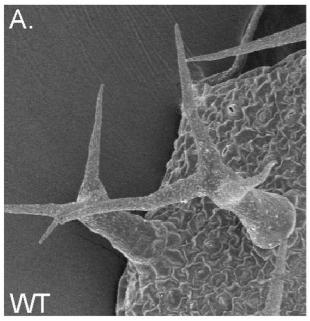

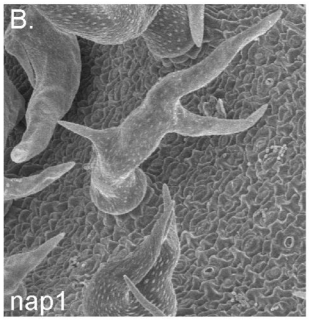

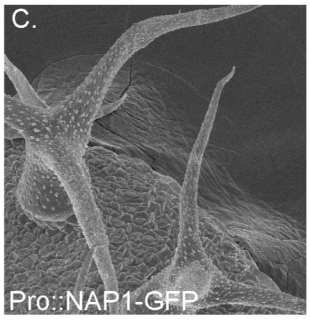

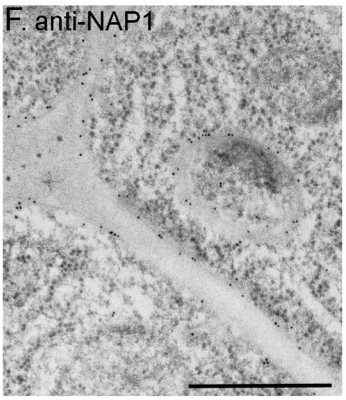

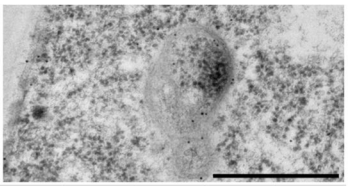

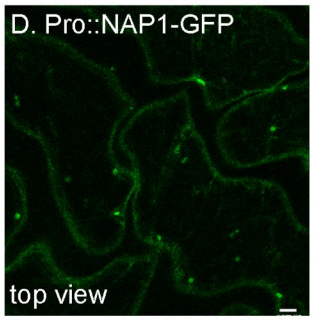

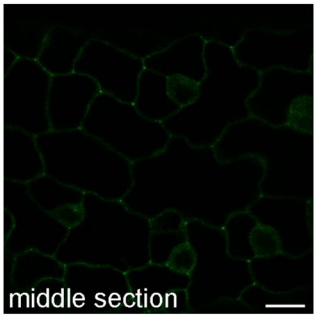

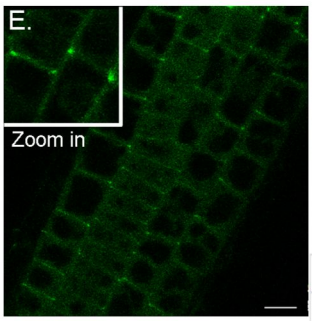

PM	Cyto	Autoph	Vesicles	ER
374	49	339	71	14

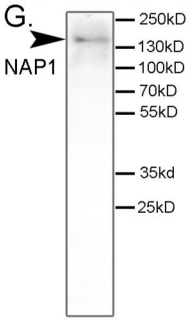

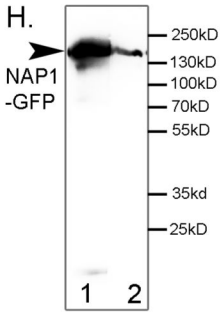

I. NAP1 enrichment

	Total Numbers	Surface area (µm2)	Proportion to total area	Density (per µm2)	Expected for random distribution	P-Value
PM associated	99	0.61	8.99%	162.30	14.29	p < 0.0001
Autophagosome associated	27	0.18	2.65%	150	4.29	P < 0.0001
Other gold particles	60	6	88.4%	10	140.6	n/a

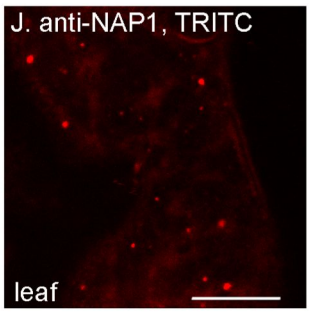

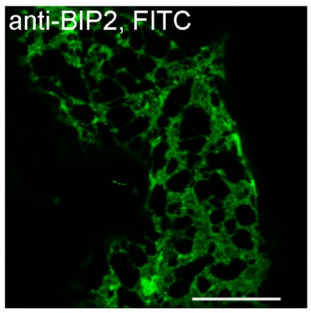

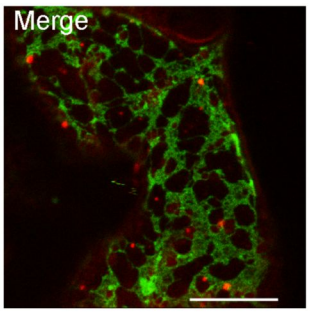

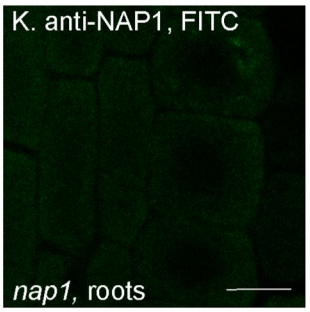

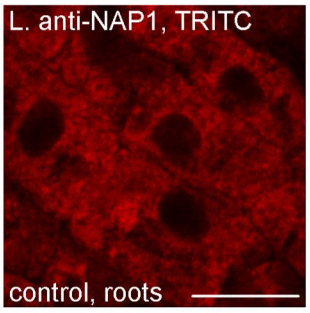

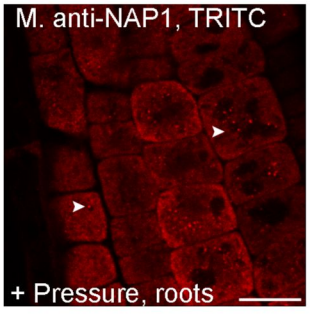

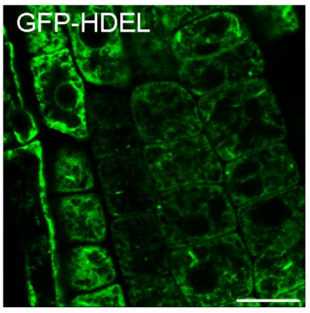

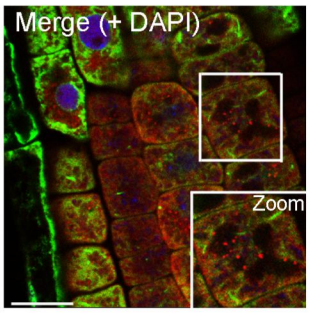

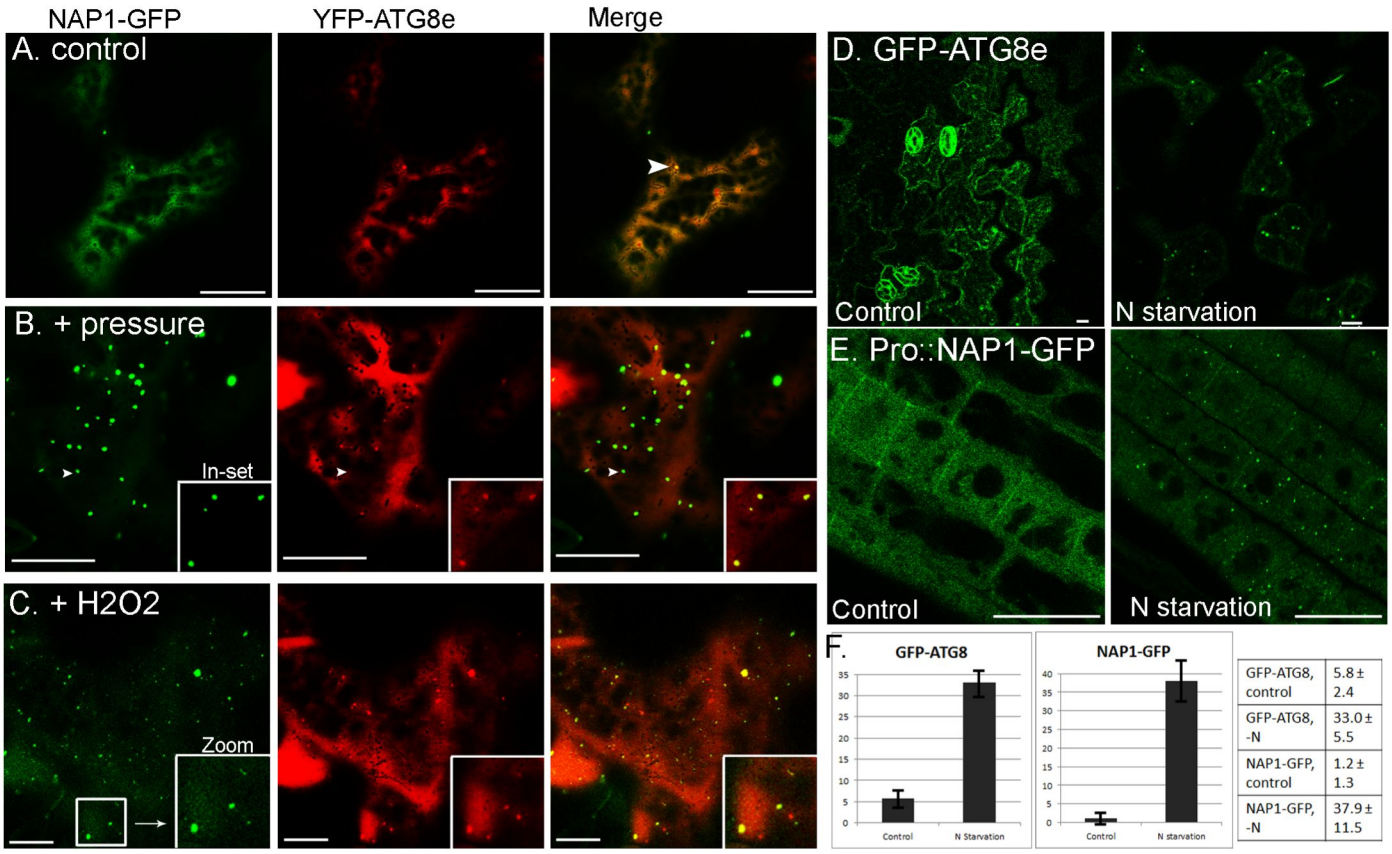
NAP1-GFP
YFP-ATG8e
Merge
A. control
B. + pressure
In-set
C. + H2O2
Zoom
D. GFP-ATG8e
Control
N starvation
E. Pro::NAP1-GFP
Control
N starvation
F.
GFP-ATG8
Control
N Starvation
NAP1-GFP
Control
N starvation
GFP-ATG8, control 5.8 ± 2.4
GFP-ATG8, -N 33.0 ± 5.5
NAP1-GFP, control 1.2 ± 1.3
NAP1-GFP, -N 37.9 ± 11.5

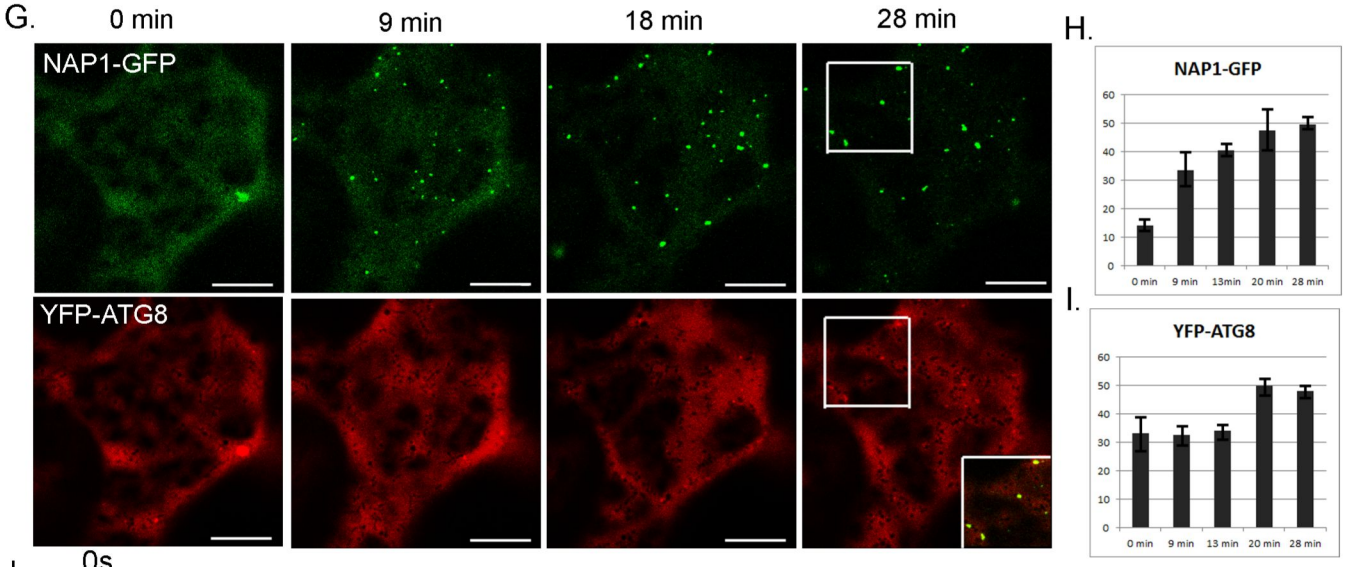
G.
0 min
9 min
18 min
28 min
NAP1-GFP
YFP-ATG8
H.
NAP1-GFP
0 min
9 min
13min
20 min
28 min
I.
YFP-ATG8
0 min
9 min
13 min
20 min
28 min

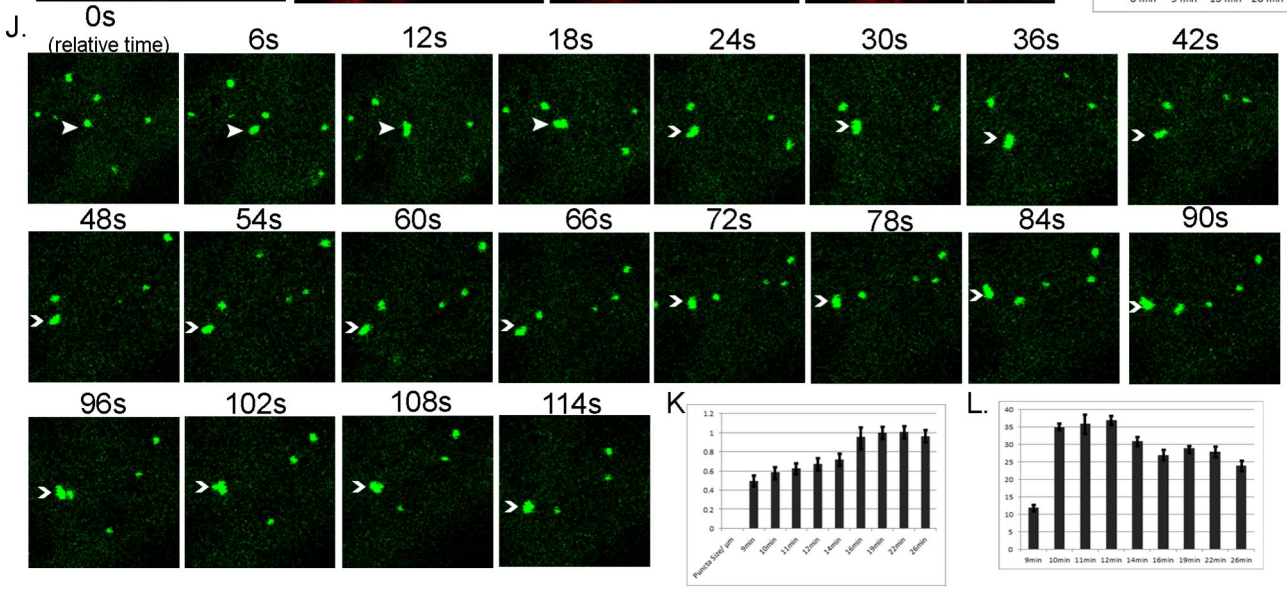
J.
0s
(relative time)
6s
12s
18s
24s
30s
36s
42s
48s
54s
60s
66s
72s
78s
84s
90s
96s
102s
108s
114s
K
L.

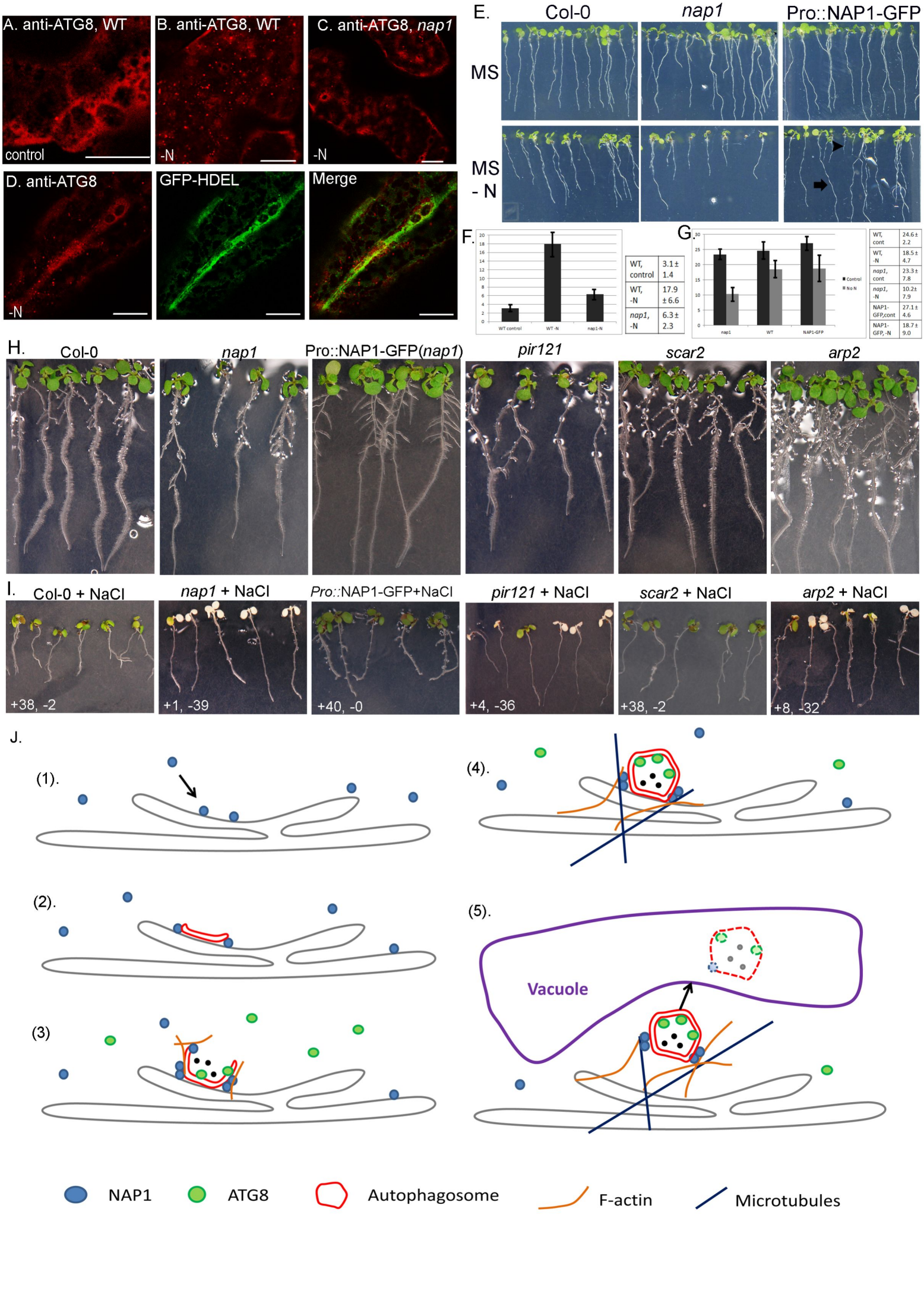
A. anti-ATG8, WT
control
B. anti-ATG8, WT
-N
C. anti-ATG8, nap1
-N
D. anti-ATG8
-N
GFP-HDEL
Merge
E.
Col-0
nap1
Pro::NAP1-GFP
MS
MS - N
F.
WT control
WT -N
nap1-N
WT, control 3.1 ± 1.4
WT, -N 17.9 ± 6.6
nap1, -N 6.3 ± 2.3
G.
Control
No N
nap1
WT
NAP1-GFP
WT, cont 24.6 ± 2.2
WT, -N 18.5 ± 4.7
nap1, cont 23.3 ± 7.8
nap1, -N 10.2 ± 7.9
NAP1-GFP,cont 27.1 ± 4.6
NAP1-GFP, -N 18.7 ± 9.0
H.
Col-0
nap1
Pro::NAP1-GFP(nap1)
pir121
scar2
arp2
I.
Col-0 + NaCl
nap1 + NaCl
Pro::NAP1-GFP+NaCl
pir121 + NaCl
scar2 + NaCl
arp2 + NaCl
+38, -2
+1, -39
+40, -0
+4, -36
+38, -2
+8, -32
J.
(1).
(2).
(3)
(4).
(5).
Vacuole
NAP1
ATG8
Autophagosome
F-actin
Microtubules

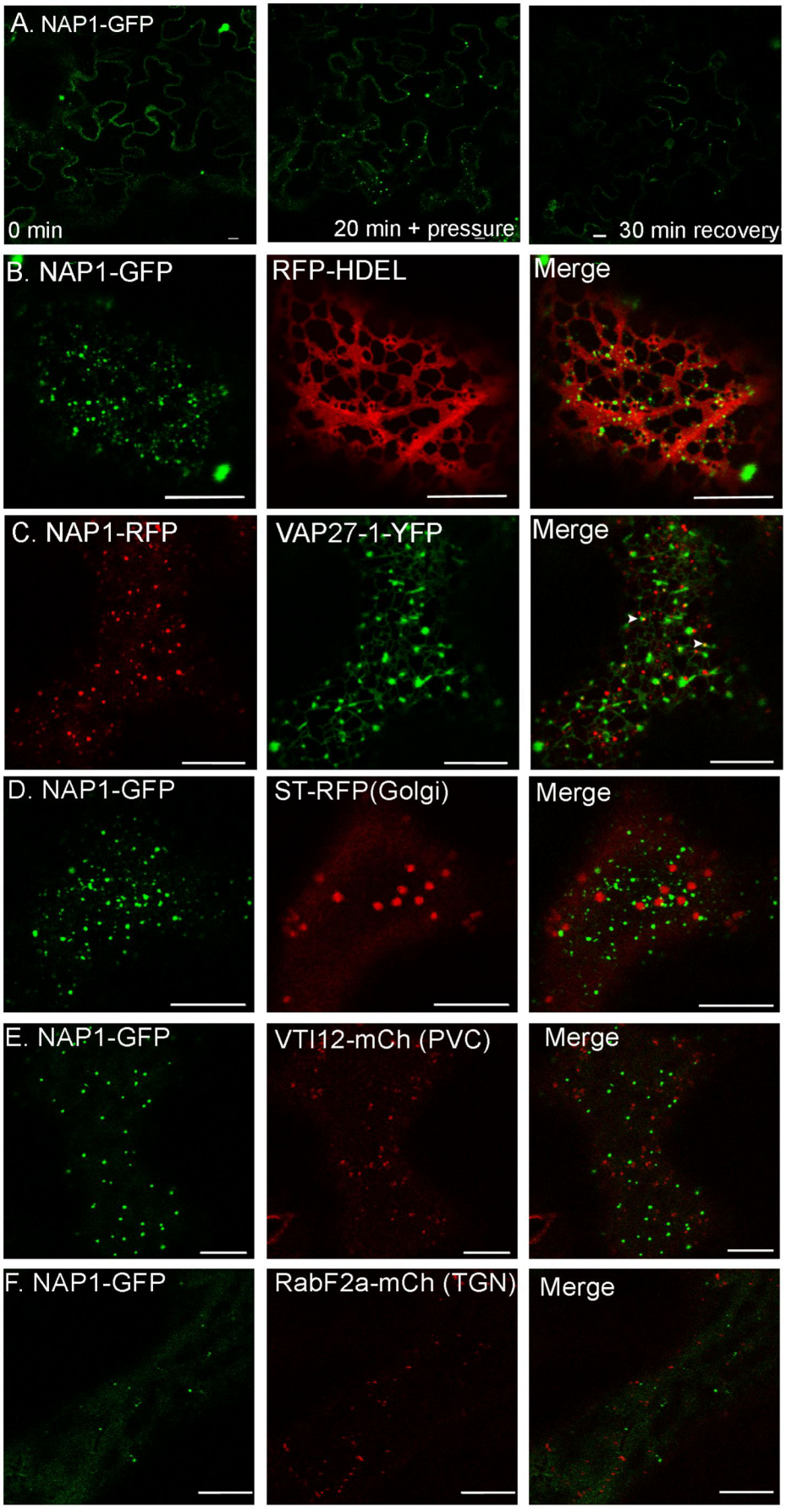
A. NAP1-GFP
0 min
20 min + pressure
30 min recovery
B. NAP1-GFP
RFP-HDEL
Merge
C. NAP1-RFP
VAP27-1-YFP
Merge
D. NAP1-GFP
ST-RFP(Golgi)
Merge
E. NAP1-GFP
VTI12-mCh (PVC)
Merge
F. NAP1-GFP
RabF2a-mCh (TGN)
Merge

Figure S1. Co-expression of NAP1-GFP/RFP with various markers in *N. benthamiana* leaf epidermal cells.

(A) The formation of NAP1 labelled puncta is reversible. Less puncta can be identified when leaf samples are released from constant pressure and recovered in water for 30min. In order to form NAP1 puncta, samples were applied with constant pressure for 20min before imaging. **(A)** NAP1-GFP puncta associate closely with ER membrane. **(B)** Most of the NAP1-GFP signal is distinct from the ER-PM contact sites (EPCS) that are labelled by VAP27-1-YFP; only a few co-localizations can be identified (arrow). No co-localization was identified between NAP1-GFP puncta and Golgi **(C)**, the pre-vacuole compartment **(D)** and the *trans*-Golgi network **(E)** (Scale bar = 10 µm). See also Figure 1.

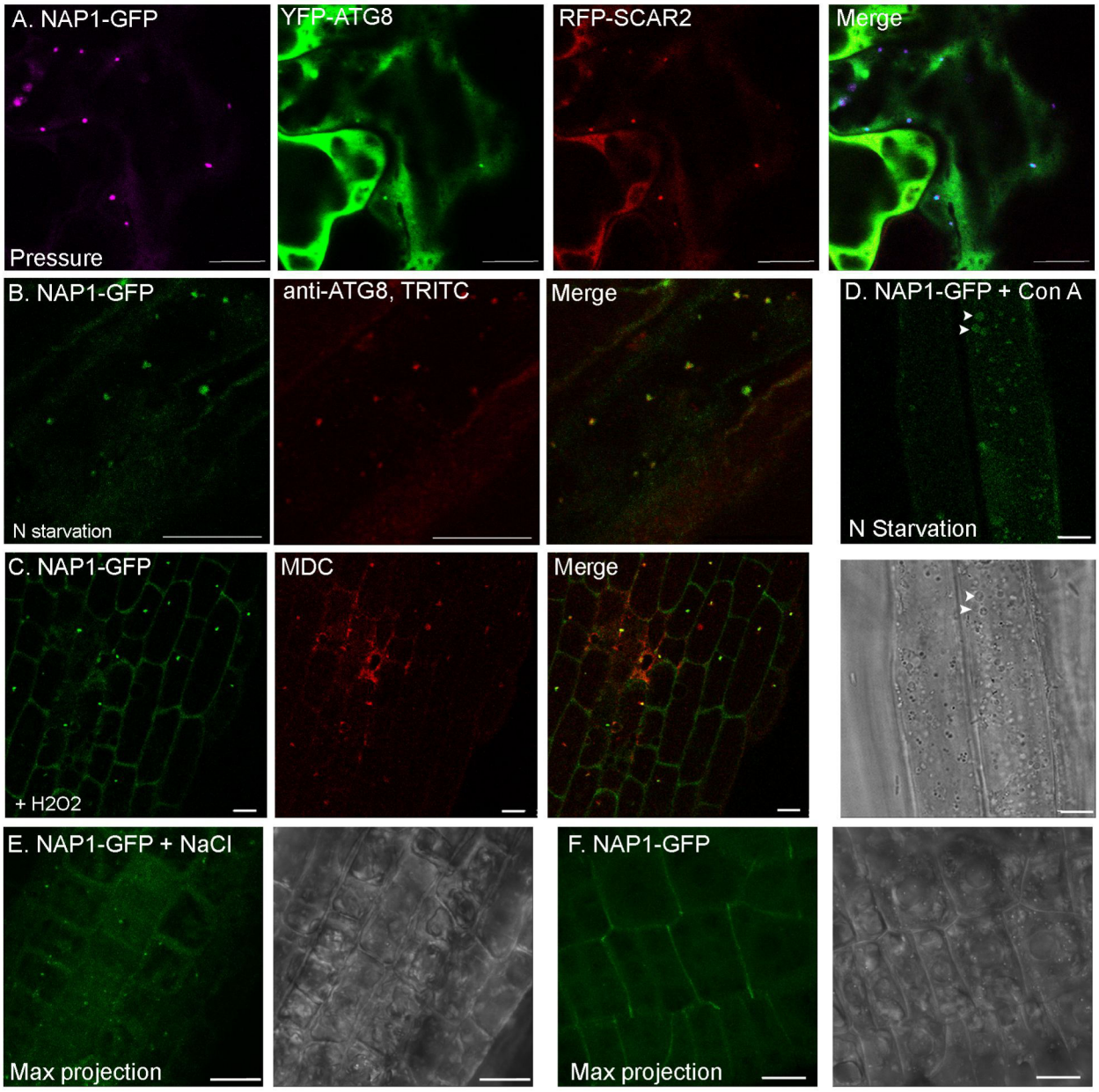
A. NAP1-GFP
YFP-ATG8
RFP-SCAR2
Merge
Pressure
B. NAP1-GFP
anti-ATG8, TRITC
Merge
D. NAP1-GFP + Con A
N starvation
N Starvation
C. NAP1-GFP
MDC
Merge
+ H2O2
E. NAP1-GFP + NaCl
F. NAP1-GFP
Max projection
Max projection

Figure S2. NAP1 labelled puncta are identified as autophagosomes.

(A) In transiently expressing *N. benthamiana* epidermal leaf cells, pressure induced NAP1-GFP puncta co-localized with the autophagosome marker (YFP-ATG8) and another SCAR complex component, RFP-SCAR2**. (B)** Arabidopsis plants expressing Pro::NAP1-GFP were grown on medium without nitrogen for two days, and fixed for immuno-fluorescence with anti-ATG8. Co-localization suggested that these puncta labelled with NAP1 are autophagosomes. **(C)** Similarly, Arabidopsis expressing Pro::NAP1-GFP were treated with H_2O_2 and stained with monodansylcadaverine (MDC), a fluorescent dye that labels autophagosomes. NAP1-GFP co-localised with MDC on the punctate structures, further confirming these puncta to be autophagosomes. **(D)** Concanamycin A (Con A) blocks the V-ATPase on the tonoplast and as a result, its function for degradation is inhibited. When NAP1-GFP plants were grown on –N medium and treated with Con A, membrane structures labelled with NAP1-GFP were found inside the vacuole (arrow), suggesting that the NAP1 labelled autophagosomes can fuse to the vacuole, where they get degraded under normal conditions. **(E-F)** NAP1 labelled autophagosomes can also be formed under salt stress (Scale bar = 10 μm). See also Figure 3.

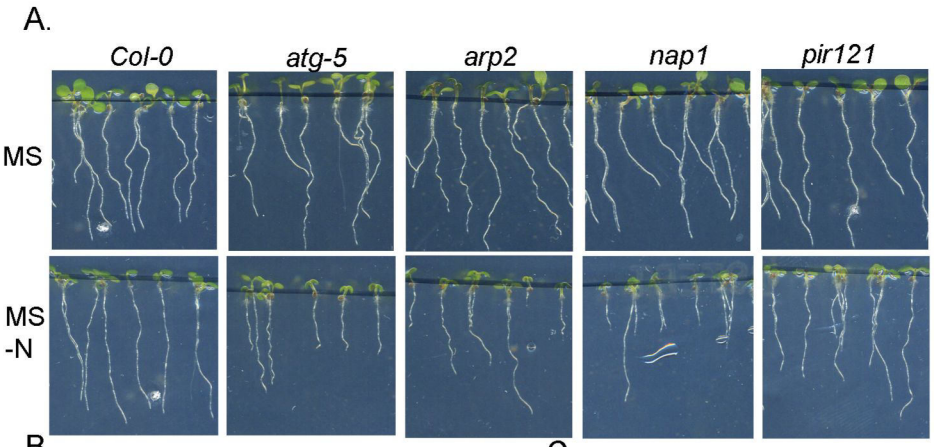

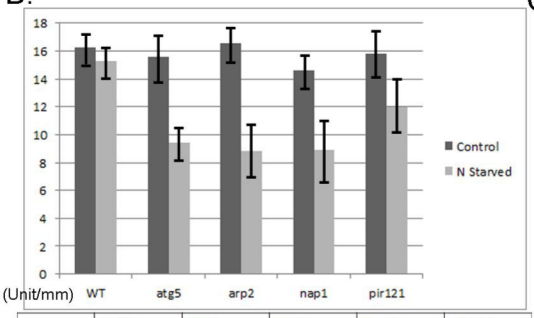

	Col-0	*atg5*	*arp2*	*nap1*	*pir121*
Control	16.25 ± 1.8	15.59 ± 3.2	16.54 ± 2.5	14.59 ± 2.7	15.8 ± 3.0
N starved	15.28 ± 2.0	9.43 ± 2.7	8.82 ± 4.0	8.88 ± 4.5	11.95 ± 3.6

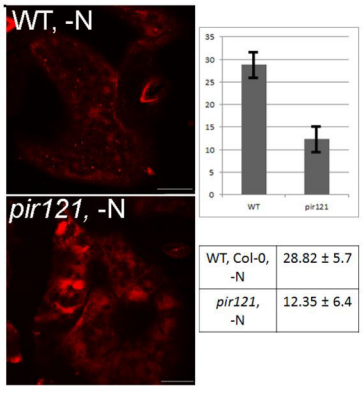

WT, Col-0, -N	28.82 ± 5.7
pir121, -N	12.35 ± 6.4

Figure S3. Arabidipsis *pir121* mutants: another example where mutation of a SCAR/WEVE complex component causes a defect in the autophagic pathway.

(A) Arabidopsis SCAR/WAVE and ARP2/3 complex mutant (*nap1, pir121 and apr2*) grown in nitrogen dropout medium exhibits slow development and shorter roots (6 days after germination). A similar phenotype is also seen in the *atg5* knock out mutant known to be , defective in autophagy. **(B)** Root length in (A) is measured and a significant reduction is seen in *atg5*, *nap1, pir121 and apr2* mutants. (C-D) Statistical analysis of the number of autophagosome formed under nitrogen starvation. For each microscopy field, 28.82 ± 5.7 autophagosomes are found in wild type, and 12.35 ± 6.4 in the *pir121* mutant (scale bar = 10 μm). See also Figure 4.

Table S1. List of Primers used in this study.

Name of Primer	Sequence (5'-3')
NAP1-F	gggg aca agt ttg tac aaa aaa gca ggc ttc ccg cca ATG GCG AAT TCT CGT CAA TAT TAT C
NAP1-R	gggg acc ac ttt gta caa gaa agc tgg gtc GTTATGCTGTTTATATGAGATGGGACC
NAP1-Promoter-F	gggg aca agt ttg tac aaa aaa gca ggc ttc ccg cca CTT GGA GAT TCT TGA TTT TGT GGTC
ARP3-F	gggg aca agt ttg tac aaa aaa gca ggc ttc ccg cca ATG GAC CCT TCT ACC TCT CG
ARP3-R	gggg acc ac ttt gta caa gaa agc tgg gtc TCA ATA CAT TCC CTT GAA TAC AGG
ATG8e-F	GGA CTT GGA TCC GGA TCT ATG AAT AAA GGA AGC ATC TTT AAG
ATG8e-R	CCG GCC GAG CTC TTA GAT TGA AGA AGC ACC GAA TGT G

Supplemental Experimental Procedures

Plant growth, treatment and transformation

Arabidopsis (Col-0) was grown on either ½ MS agar (1% Sucrose, pH 5.6) or compost in a growth chamber with 16hr light (22 °C) and 8hr darkness (18 °C). Stable Arabidopsis lines were transformed by floral-dipping as described in Zhang et al. [S1]. *Nicotiana benthamiana* was kept in a growth room with 16hr light (25°C) and 8hr darkness (18°C). Transient expression was performed by leaf infiltration according to Sparkes et al. [S2]. Nitrogen starvation induced autophagy was performed by transferring 5-6 day old seedlings to nitrogen-free MS plates for 24-48 hours before imaging. Concanamycin A (Con A) treatment was performed by transferring N starved seedlings to medium containing 1µM Con A for a further 12 hours. Medium containing ½ MS agar and 160mM NaCl was used for salt stress; plants were first grown on normal medium for 5 days and then transferred onto these medium. For the plant development study, sterilized seeds were grown on vertical plates containing either MS medium or MS medium without nitrogen. Root length was measured 6-7days after germination using ImageJ. Arabidopsis SCAR complex mutants used in this study have been characterized and described in previous studies; *nap1* [S3], *scar2* [S4], *pir121* [S5]. They were grown together with wild type and harvested at the same time for phenotypical analysis.

Molecular cloning

The cDNAs of NAP1 were amplified from 10 day old Arabidopsis seedling RNA by RT-PCR (Invitrogen), and cloned into pMDC83 (C-terminal GFP or RFP) plasmid using Gateway reactions (Invitrogen). The NAP1 gene (genomic sequence including 2Kb upstream of ATG) was amplified by PCR and cloned into pMDC107 for endogenous expression of the GFP chimera. Primers used for cloning full length NAP1 are listed in Table S1. A cDNA fragment corresponding to the NAP1 peptide (N-terminal 1-89 aa) used as an antigen in mice was cloned into the NheI/HindIII sites of pET28a vector (with N-terminal HisTag) for *in-vitro* protein expression in *E.coli* (Rosetta 2, Novagen). ATG8e described in [S6] was sub-cloned into pVKHEn6 vector (N-terminal YFP) at the BamH1 and Sac1 restriction sites. NtARP3 described in [S7] was sub-cloned into pMDC43 (N-terminal RFP) by Gateway.

Antibodies and immunofluorescence

Antigen peptide of NAP1 (residue 1-89, N-terminal sequence) was expressed and purified using nickel agarose beads (Qiagen). Polyclonal antibodies were raised in mice as described in Smertenko et al. [S8]. Immunofluorescence studies were performed as described in Wang 2014. Root tips were fixed in 4% PFA and 0.01% glutaraldehyde, in PIPES buffer (0.1M PIPES pH6.9, 1mM MgSO4, 2mM EGTA) for 60min followed by Driselase (2%) digestion for 7min. Samples were treated with 0.1% Triton for 5min and incubated in primary and secondary antibody for 3 hours or overnight at 4°C. Freeze shattering and immunofluorescence of leaf cells was performed as described in [S9]. Anti-NAP1, anti-BIP2 (Agrisera) and anti-ATG8 [S10] antibodies were used at 1:100-1:200 dilutions, followed by secondary antibody incubation with TRITC or FICT-conjugated secondary antibody at 1:200 dilution (Jackson ImmunoResearch).

Live cell imaging and drug treatment

Transiently transformed *N. benthamiana* were imaged two days after infiltration using a laser scanning confocal microscope (LSCM, Leica SP5). Images were taken in multi-track mode with line switching when multi fluorescence was used. Normally, pictures were taken within 5min after mounting to avoid prolonged pressure. When constant pressure is required, samples were left in mounting water with cover slips on, and pictures were taken at different times as indicated. For the water dipping lens, the experiment was performed using an upright Zeiss Meta510Meta confocal microscope. Samples were fixed on the bottom of a petri-dish, and imaged through water.

Electron microscopy and immune-gold labeling

For TEM study, Arabidopsis roots were fixed by high-pressure freezing with freeze substitution as described in Deeks et al. [S11]. NAP1 anti-serum was used at 1:50 dilution and detected by 5nm gold-conjugated goat anti mouse antibody. For SEM the small first leaves were fixed overnight in 2% paraformaldehyde, 2.5% glutaraldehyde in 0.1M sodium cacodylate buffer pH 7.4. After rinsing with 0.1M sodium cacodylate buffer, fixation continued in 1% osmium tetroxide in 0.1M sodium cacodylate buffer pH 7.4 for 2hrs. The

leaves were then dehydrated, critical point dried, attached to silicon chips and coated with 5nm of platinum before viewing with a Hitachi S5200 FESEM at 10kV.

Western blotting

Protein extracts were heated to 95°C in SDS buffer. Samples were loaded onto a 12.5% SDS-gel followed by electrophoresis and protein transfer to nitrocellulose membrane. For detection, the membrane was incubated in 2xTBST buffer with 5% milk prior to primary antibody incubation (1:200 for anti-NAP1; 1:500 for anti-GFP) at room temperature for 3 hours. After three washes in TBST buffer, the membrane was probed with HRP-conjugated mouse secondary antibody (1:3000) and developed using an ECL reagent (GE heathcare).

Chi-square and statistical analysis

In order to confirm that the association between anti-NAP1 gold and the PM or autophagosome are not a coincidental event, chi-square tests were applied. The area of plasma membrane and autophagosome were measured. The distribution of anti-NAP1 gold scored as PM/autophagosome-associated or non-associated. The p value was calculated based on the real distribution of anti-NAP1 compared to the expected number from a random distribution.

Supplemental References

S1. Zhang, X., Henriques, R., Lin, S.S., Niu, Q.W., and Chua, N.H. (2006). Agrobacterium-mediated transformation of Arabidopsis thaliana using the floral dip method. Nature protocols *1*, 641-646.

S2. Sparkes, I.A., Runions, J., Kearns, A., and Hawes, C. (2006). Rapid, transient expression of fluorescent fusion proteins in tobacco plants and generation of stably transformed plants. Nature protocols *1*, 2019-2025.

S3. Deeks, M.J., Kaloriti, D., Davies, B., Malho, R., and Hussey, P.J. (2004). Arabidopsis NAP1 is essential for Arp2/3-dependent trichome morphogenesis. Curr Biol 14, 1410-1414.

S4. Uhrig, J.F., Mutondo, M., Zimmermann, I., Deeks, M.J., Machesky, L.M., Thomas, P., Uhrig, S., Rambke, C., Hussey, P.J., and Hulskamp, M. (2007). The role of Arabidopsis SCAR genes in ARP2-ARP3-dependent cell morphogenesis. Development 134, 967-977.

S5. Li, Y., Sorefan, K., Hemmann, G., and Bevan, M.W. (2004). Arabidopsis NAP and PIR regulate actin-based cell morphogenesis and multiple developmental processes. Plant physiology 136, 3616-3627.

S6. Contento, A.L., Xiong, Y., and Bassham, D.C. (2005). Visualization of autophagy in Arabidopsis using the fluorescent dye monodansylcadaverine and a GFP-AtATG8e fusion protein. Plant J 42, 598-608.

S7. Maisch, J., Fiserova, J., Fischer, L., and Nick, P. (2009). Tobacco Arp3 is localized to actin-nucleating sites in vivo. J Exp Bot 60, 603-614.

S8. Smertenko, A.P., Kaloriti, D., Chang, H.Y., Fiserova, J., Opatrny, Z., and Hussey,P.J. (2008). The C-terminal variable region specifies the dynamic properties of Arabidopsis microtubule-associated protein MAP65 isotypes. Plant Cell 20, 3346-3358.

S9. Wang, P., Richardson, C., Hawkins, T.J., Sparkes, I., Hawes, C., and Hussey, P.J. (2016). Plant VAP27 proteins: domain characterization, intracellular localization, and role in plant development. New Phyt, DOI: 10.1111/nph.13857

S10. Ketelaar, T., Voss, C., Dimmock, S.A., Thumm, M., and Hussey, P.J. (2004). Arabidopsis homologues of the autophagy protein Atg8 are a novel family of microtubule binding proteins. FEBS Lett 567, 302-306.

S11. Deeks, M.J., Calcutt, J.R., Ingle, E.K., Hawkins, T.J., Chapman, S., Richardson, A.C., Mentlak, D.A., Dixon, M.R., Cartwright, F., Smertenko, A.P., et al. (2012). A superfamily of actin-binding proteins at the actin-membrane nexus of higher plants. Curr Biol 22, 1595-1600.